



**HAL**  
open science

## A software receiver for GPS-IIF L5 signal

Lionel Ries, Christophe Macabiau, Olivier Nouvel, Quentin Jeandel, Willy Vigneau, Vincent Calmettes, Jean-Luc Issler

► **To cite this version:**

Lionel Ries, Christophe Macabiau, Olivier Nouvel, Quentin Jeandel, Willy Vigneau, et al.. A software receiver for GPS-IIF L5 signal. ION GPS 2002, 15th International Technical Meeting of the Satellite Division of The Institute of Navigation, Sep 2002, Portland, United States. pp 1540 - 1553. hal-01021711

**HAL Id: hal-01021711**

**<https://enac.hal.science/hal-01021711v1>**

Submitted on 30 Oct 2014

**HAL** is a multi-disciplinary open access archive for the deposit and dissemination of scientific research documents, whether they are published or not. The documents may come from teaching and research institutions in France or abroad, or from public or private research centers.

L'archive ouverte pluridisciplinaire **HAL**, est destinée au dépôt et à la diffusion de documents scientifiques de niveau recherche, publiés ou non, émanant des établissements d'enseignement et de recherche français ou étrangers, des laboratoires publics ou privés.

# A Software Receiver for GPS-IIF L5 Signal

Lionel Ries, CNES, C. Macabiau, ENAC/TéSA, O. Nouvel, Q. Jeandel, W. Vigneau, M3Systems,  
V. Calmettes, Supaero/TéSA, J.L. Issler, CNES

## BIOGRAPHY

Lionel Ries is a Navigation Engineer in the Radionavigation Departement at CNES (French Space Agency), since June 2000. He studies GNSS2 signal including BOC and GPSIIF-L5. In addition, he is involved in experiments on a GNSS2 navigation payload demonstrator (developed by CNES). He formerly worked for Altran, as consultant (Astrium, Toulouse and Allgon Stockholm, Sweden). He graduated in 1997 from the "Ecole Polytechnique de Bruxelles, at Brussels Free University" (Brussels, Belgium), in 1997, and received a M.S. degree from the "Ecole Nationale Supérieure de l'Aéronautique et de l'Espace" (Supaero, Toulouse, France).

Christophe Macabiau graduated as an electronics engineer in 1992 from the ENAC (Ecole Nationale de l'Aviation Civile) in Toulouse, France. Since 1994, he has been working on the application of satellite navigation techniques to civil aviation. He received his Ph.D. in 1997 and has been in charge of the signal processing lab of the ENAC since 2000.

Willy Vigneau is responsible of the RadioNavigation Unit of M3 Systems, an SME located near Toulouse (France) which provides services in the Space and Aeronautic domains and is closely involved in RadioNavigation projects related to GPS, EGNOS and GNSS2. Olivier Nouvel is particularly involved in interferences study between GPS and Galileo in support for CNES. Quentin Jeandel is specialized in the modelling and simulation of RadioNavigation receivers and in particular the L5 software receiver development.

Vincent Calmettes is a research Engineer at SUPAERO (Toulouse, France), leading the research group "Signals, Communications and Navigation" and teaching signal processing and communications. His work includes the research, for applications in Digital communications and Signal processing, of solutions with DSP and PLDs or ASICs

Jean-Luc Issler is head of the RadioNavigation Department at CNES, whose main task are signal processing and radio-navigation equipments. He is involved in the development of several GNSS spaceborne

receivers in Europe, as well as studies on the future European RadioNavigation Programs, like Galileo and the pseudolite network.

## ABSTRACT

The block IIF of the GPS will feature a new civil signal, with a bandwidth of 24 MHz. The first launch is scheduled for 2005 and the full operational availability around 2012. This new L5 signal is QPSK-modulated, centered on 1176.45 MHz. Its two components have each a different spreading code at 10.23 Mcps. The in-phase component carries the navigation message, at 100 symbols per second (50 bits per second with a convolutional encoder) while the quadrature component, called the pilot channel, carries no message at all. The specified power is such that the received levels on the ground should be  $-154$  dBW (i.e.  $-157$  dBW for each component).

In order to closely study the L5 signal, as well as to improve expertise on QPSK radio-navigation signals, CNES (the French Space Agency) has undertaken the development of simulation bench, including a software receiver. This tool comprises a L5 signal generator coupled to a L-band digitizer and a signal processing software, comparable to a software receiver. CNES has chosen this approach not only because it provided a flexible simulation tool for L5 (and any other QPSK radio-navigation signal), but also in order to develop its own capability and expertise in the field of software receiver for radio-navigation signals. The L5 codes and receivers are also studied by ESA, DSTL, UniBW and STNA for instance.

This paper presents the work of CNES in the area of software receiver and especially to provide and discuss some interesting results about the L5 signal. First of all, a theoretical analysis of the L5 spreading codes is summarized, showing some little discrepancies in the codes specifications. Since the GPSIIF-L5 signal will share the same band as Galileo E5a, also a QPSK-like signal, the paper presents a methodology to evaluate the interference of one system on another. The objective is to assess the RF compatibility between GPS and Galileo E5a signals.

The theoretical analysis is pursued on the software receiver ( using simulated input signals ) to evaluate the acquisition and tracking performances one can expect from the signal. In particular, the use of the pilot channel and its impact on the loop organization (DLL, PLL & FLL) is put in evidence. The complete simulation bench is presented.

The main results of these simulations are synthetized and discussed. Their comparisons with the theoretical assessments, both in tracking and acquisition, have allowed not only the tool's validation but also to verify some signal processing. The acquisition and tracking performances of those receivers are being compared with those of equivalent L1 C/A receiver, especially in the case of low signal to noise density ratio.

Finally, an application example of L5 processing, outside the scope of aeronautic, is given. The case of a L5 receiver in GEO/GTO orbit is analyzed. It provides a sensible improvement of the tracking and acquisition capacity.

## INTRODUCTION

The L5 signal radiated by satellite  $i$  is a QPSK modulation of the L5 carrier with a data and a pilot channel that can be modeled as :

$$S_{L5}^i(t) = A d^i(t) NH_{10}(t) XI^i(t) \cos(2\pi f_s t) + ANH_{20}(t) XQ^i(t) \sin(2\pi f_s t)$$

where :

$A$  is such that the minimum total power of the received L5 signal is  $-154$  dBW, or  $-157$  dBW for each one of the data and pilot component [1].

$d$  is the P/NRZ/L materialization of the L5 navigation message encoded with a Viterbi FEC. The original L5 navigation message has a 50 Hz rate, while  $d$  has a final 100 Hz rate after Viterbi encoding. Thus the duration of one final symbol in  $d$  is 10 ms.

$NH_{10}$  and  $NH_{20}$  are respectively the P/NRZ/L materialization of a 10 bits and 20 bits Neuman-Hoffman code. These codes are clocked at a rate of 1 kHz, thus the duration of one bit is 1 ms.

$XI$  and  $XQ$  are respectively the P/NRZ/L materialization of the data and pilot component PRN codes. Those codes are clocked at a rate of 10.23 MHz and have a period of 1 ms.

Figure 1 illustrates that model [2], [3].

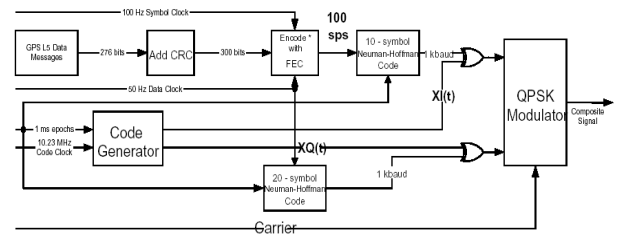


Figure 1. Present GPSIF-L5 signal structure

## THE SOFTWARE RECEIVER

The software receiver was developed using SPW© (Signal Processing Workshop) from Cadence. It allows for two types of simulation processes :

one using only software computation, both signal generation and receiver signal processing are performed by SPW,

one hybrid mode, where the L5 signal is hardware generated and digitized before uploading for processing by SPW.

Both mode uses the same signal processing at reception.

### Full software simulation

The signal is generated by the software simulator, enabling all kinds of relative dynamics between the satellite and the receiver. Moreover, the channel can model ionosphere, DME, multipath, etc.

The signal transmitter includes all the baseband functions required for signal generation. It allows for satellite motion and reference clock drift simulation.

The channel blocks include the following : signal attenuation, multipath, CW and DME jammers, ionosphere, among other types of perturbations.

The software receiver was developed taking the most benefit of SPW graphical interface and block functions. This allows to simulate any existent receiving architecture as well as to design new architecture, optimized for data and pilot channel processing.

### Mixed hardware/software simulation

The software receiver is also able to process real digitized signal. For that purpose, the present L5 signal is hardware generated in a FPGA coupled to a modulator, and then digitized using an adequate Bitgrabber. The saved samples are then uploaded onto the processing workstation for further processing by SPW.

### Signal generator

It includes a digital signal generator implemented in a FPGA and a parametric RF signal generator/modulator from Rhode & Schwarz. They share the same reference clock, providing the required synchronization between code and carrier.

The FPGA's inputs include two 13 bits words setting the codes, and the chip rate as reference clock.

The modulator allows the setting of:

- the carrier's frequency and level,
- the carrier's Doppler sweep,
- if necessary, the modulator can apply baseband filtering on the digital streams including SRC and Gaussian filter for instance.

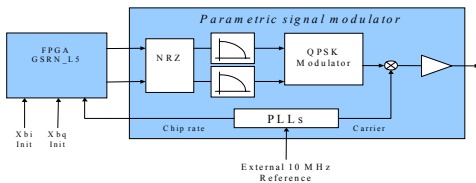


Figure 2. Signal generator

### Bitgrabber and software processing

In order to avoid the development of a dedicated L5 front-end, we decided to use an off-the-shelf L1 digitizing front-end. The immediate consequence is a generated signal transmitted at L1 instead of L5.

The collected samples are then stored on a PC hard disk (see Figure 3), called the data-logger, prior to be uploaded on the processing workstation.

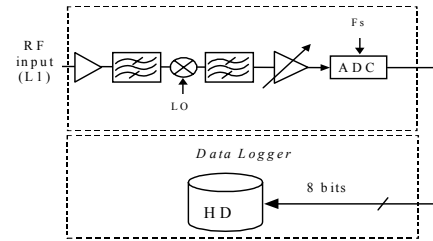


Figure 3 Digitizing Front-end & Data-logger

### L5 SIGNAL PROPERTIES

#### Spreading code properties [6]

The XI & XQ codes are PN-sequences generated using 13 bits registers. Their truncated length is 10230 chips.

The computation of those PN codes auto-correlation function (ACF) on 1 ms, leads to the properties reported in Table 1. These values can be compared to the Welsh bound and to the margin of full length Gold codes which are far better, respectively  $-40$  dB and  $-36$  dB. The explanation is that the L5 codes are truncated sequences, and thus provide lower correlation margin.

Table 1. Correlation properties of L5 PN codes

Property	XI( data)	XQ (pilot)	L1 C/A
Max Auto-correlation	-29.2 dB	-29.0 dB	-23.9 dB
Max cross-correlation	-26.4 dB	-26.5 dB	-23.9 dB
Max cross-correlation (Xi(n) /XQ(m))		-26.4 dB	NA

However, the theoretical margin for truncated sequence is  $-30.2$  dB, close to the results of the L5 codes. So, as truncated Gold sequence, the L5 code family can hardly be better. But other code families could reach lower values and come closer to the Welsh Bound. This is what must be sought for the Galileo E5a codes in the frame of a global optimization of GPS and Galileo code families in E5a.

The isolation between each XI and XQ pair is specified at  $-74.2$  dB. When starting our analysis in November 2001, we discovered that 3 pairs of codes were not properly defined since the following sequences were identical (sharing the same initialization word) :  $14 = Q34$ ,  $117=Q37$  and  $129=Q32$  [13], [6].

After we reported the fact to the specifying authorities of the L5 signals, three new codes were defined for XQ, resulting now in an isolation bound of  $-62$  dB. The other properties were not affected by the change in code specification.

## Neuman-Hoffman and tiered code properties

The Neuman-Hoffman sequences extend the performances of XI and XQ. Indeed, they lower the spectrum line by 10 or 13 dB (10 dB for the data channel, and 13 dB for the pilot channel) and provide effective longer codes, called tiered codes.

Since the Neuman-Hoffman sequences and the PN codes are independant, the tiered codes ACF is the product of the Neuman-Hoffman ACF and the PN codes ACF on 20 ms.

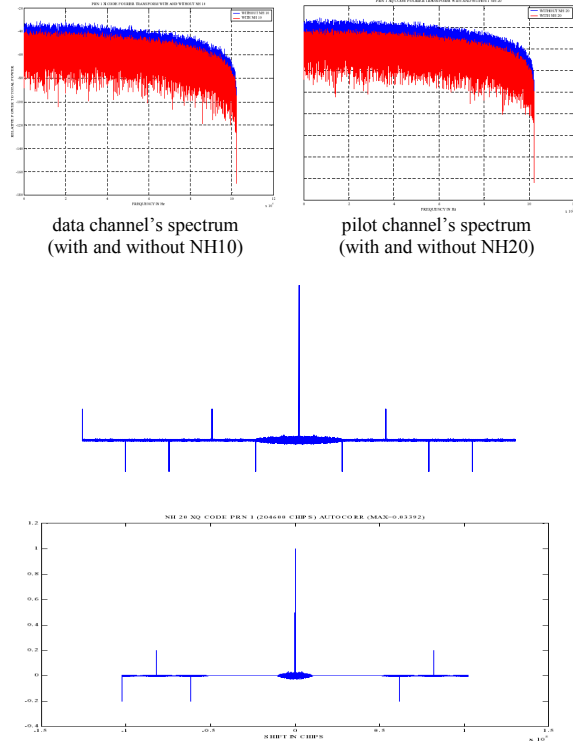


**Figure 4 Spectrum and Auto-correlation functions of data and pilot tiered codes (10 ms and 20 ms)**

The general aspect of the 20 ms ACF brings the following remarks :

within 1 ms of the main peak, the ACF has a standard shape, close to the one of the PN sequences. The correlation margin is around  $-28$  dB,

as the relative delay increases , we see several secondary lobes appearing, with levels reaching  $-14$  dB ( 0.2 amplitude).

In presence of Doppler uncertainty, these secondary lobes can come within 6 dB of the main peak. In itself, this is not surprising, since the NH sequence is short. But, it can be a limitation when computing acquisition because of the locking probability onto secondary lobes, missing the bit synchronization.

**Table 2. Correlation properties of L5 tiered codes (incl. NH)**

Property	XI( data)	XQ (pilot)	L1 C/A
Max Auto-correlation	-29.8 dB	-29.4 dB	-23.9 dB
Max Cross-correlation	-28.1 dB	-28.5 dB	-23.9 dB
Max Cross-correlation XI(n)/XQ(m)	-33.3 dB		

## RF COMPATIBILITY IN E5A/L5

### Assessing the radio-frequency compatibility between two multi-signals systems sharing the same frequency

A receiver dedicated to one system will observe interference of both systems. This could be caused by its own system (intra-system interference) and by the second system (inter-system interference).

The intra-system and inter-system interference powers are noted respectively  $I_{INTRA}$  and  $I_{INTER}$ . The total interference power is the sum of the two interference components:

$$I_{TOTAL} = I_{INTRA} + I_{INTER}$$

Therefore, the equivalent signal to noise is equal to:

$$[C / No]_{eq} = \frac{C}{No + I_{TOTAL}} = \frac{C}{No + I_{INTRA} + I_{INTER}}$$

The inter-system interference carrier-to-noise degradation, called the inter-system degradation is described by:

$$(C / No)_{deg_{INTER}}(dB) = \frac{C}{No + I_{INTRA}}(dB) - \frac{C}{No + I_{INTRA} + I_{INTER}}(dB)$$

For a given time and “useful” signal, a user of the first system will suffer from the inter-system degradation noted:

$$(C / No)_{deg_{INTER}}(dB) = 10 . LOG_{10} \left( 1 + \frac{I_{INTER}}{No + I_{INTRA}} \right)$$

In the general case, the two parameters  $I_{INTRA}$  and  $I_{INTER}$  will vary as a function of time (SV visibility, signals power), user localization (antenna pattern, Doppler shifts), and codes properties (useful and interfering signals).

$No$ , the system noise is usually a constant value depending on the environment, including the antenna and the receiver itself. For instance,  $No = -201.5$  dBW/Hz is usually taken for interference analysis in L5 (1176.45 MHz).

## Proposed methodology on L5 (1176.45 MHz)

### A- Interference Coefficient

The Interference Coefficient is defined using the following :

$$Coeff = \int DSP_u(\omega) \times DSP_i(\omega) d\omega$$

Manipulations of this latter leads to the understated expressions (where  $F(\dots)$  is the Fourier Transform)

$$Coeff = \int \left| F(code_u) \times F^*(code_u) \right| \cdot \left| F(code_i) \times F^*(code_i) \right| d\omega$$

$$Coeff = \int F(ACF_u) \times F(ACF_i) d\omega$$

$$= \int \left| F(ICF_{u,i}) \right|^2 d\omega = \int DSP(ICF_{u,i}) d\omega$$

Yielding :  $Coeff = Power(ICF(\omega))$

with ICF being the inter-correlation function of code 1 and code 2. These relations show clearly the effects of useful and interfering code properties (ACF and ICF).

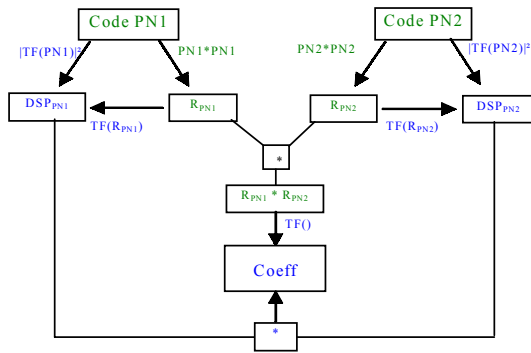


Figure 5 ACF and interference Coefficient relationship

Once the interference coefficients are known, it becomes possible to compute the total Intra-system interference and the Inter-system interference for a given useful link  $u$  :

$$I_{intra} = \sum_{i \neq u} ReceivedPower_{SV(i)} \cdot Coeff(\omega(u) - \omega(i))$$

$$I_{inter} = \sum_j ReceivedPower_{SV(j)} \cdot Coeff(\omega(u) - \omega(j))$$

where :

$i$  is the index of the intra-system satellites,

$j$  is the index of inter-system satellites,

and  $\omega/2.\pi$  are the Doppler frequencies seen by user.

The satellites powers and relative Doppler seen from a given user at a given time are computed using constellations tools like Visualize® or Satellite Tool Kit®.

### B- Signals sources models

To obtain a realistic representation of the interference events between GPS and Galileo, it has been chosen to use time dependent simulations taking into account the relative geometrical distribution and the motions of the various signals sources. GPS L5 codes (I & Q) are considered with 24 SVs<sup>1</sup> and Galileo E5a codes with 30 SVs<sup>2</sup>.

### C- Signals models

Signals are represented by their real spectrum, obtained by the fast Fourier transform of the actual codes sequences. For GPS, real L5 codes are used. For Galileo, 10230 chips random codes were used. Computations of both inter and intra-system interference powers are based on the use of interference coefficients as defined and used in [7, 8, 9]. The spectral representation of the interfering and useful signals on L5 frequency is described in Figure 6

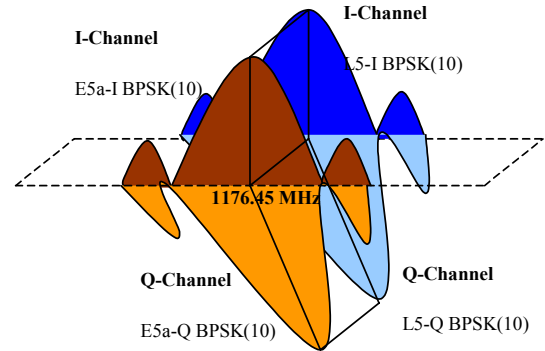


Figure 6 Spectral illustration between Galileo E5a and GPS on L5 band

### D- User description

In this simulation, user localization is on earth with: latitude: 20° and longitude: 0°. This gives an order size of inter-system degradation but not worst case values.

### E- Proposed analysis

We will analyze both inter-system degradation : Galileo on GPS and GPS on Galileo.

With a first method, we consider GPS L5 signals as a binary phase shift keying (BPSK) at 10.23 Mcps with a ground power of -154 dBW at 5° of elevation and Galileo

<sup>1</sup> Walker(24,6,2)

<sup>2</sup> 30 satellites, 3 orbital planes, 0° phase between adjacent planes.

E5a signals as a BPSK at 10.23 Mcps with a ground power of -155 dBW at 10° of elevation.

In a second method, we consider GPS L5 signals as a quadrature phase shift keying (QPSK), L5-I & L5-Q with a ground power of -157 dBW for each components and a Galileo QPSK E5a-I & E5a-Q with a ground power of -158 dBW for each components.

GPS L5-I code is generated with 10 ms Neuman-Hoffman (N-H) code with data at 100 Hz and GPS L5-Q code with 20 ms N-H code only.

Galileo E5a-I is generated with 10230 chips code with data at 25 bps (or 50 sps) and E5a-Q with 10230 chips long code only.

### Simulations results

#### A- Simulations characteristics

We assume that GPS and Galileo satellites used iso-flux antenna on L5 : their gain pattern is identical to that of L1. User's antenna is an omni-directional patch antenna with a masking angle fixed to 5°.

#### B- Results

Reminding that these simulations results are real case for a fixed user localization terminal, the following results are not worst case values of inter-system degradation.

Depending on the user location, the relative Doppler frequencies may vary, generating more or less spectrum line collision and so increasing and decreasing the overall interference.

Usually, the interference are computed using the following approximation : the signals are defined as BPSK(10) signals, with an equivalent power to the QPSK(10) signals. The approximation is justified by the lower computation it requires.

The following table summarizes the mutual inter-system degradation GPS on Galileo and Galileo on GPS in the case of BPSK(10). The results are illustrated on figure 7.

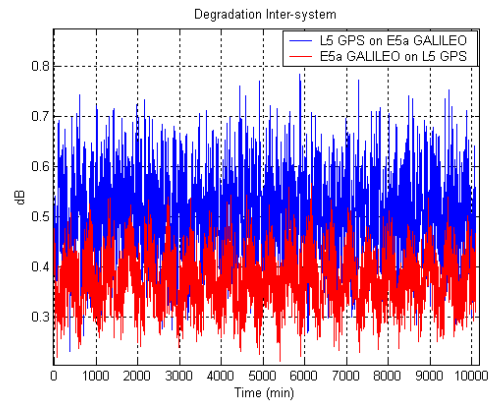


Figure 7 Mutual inter-system degradation

Table 3. Inter-system degradation (BPSK)

Inter-system degradation	Max	Min	Mean
E5a GALILEO on L5 GPS	0,56	0,21	0,37
L5 GPS on E5a GALILEO	0,78	0,23	0,5

#### C- Analysis of the results

Th results show that the inter-system degradation induced by GPS on Galileo is the most important with a maximum inter-system degradation to 0.8 dB.

The inter-system degradation created by Galileo on GPS in L5/E5A is about 0.4 dB and with peak of about 0.56 dB. These results highlighted that L5/E5A compatibility issue has to be assessed more deeply since a coordination appears to be necessary for GPS-L5 to overlay E5a. The optimization of a GPS and Galileo E5a code family could solve this problem.

### SIGNAL ACQUISITION

Many strategies can be used to implement signal detection and acquisition, but they fall in two main categories :

Either a single component acquisition, typically, the pilot channel (longer acquisition period).

Either dual component acquisition, when both the data and the pilot channel are processed, and the energy summed.

At first glance, the second strategy may seem more complex to implement , because it requires twice the amount of correlators. But since those are available in hardware because of tracking, they can also be used for

acquisition, thus increasing the available energy and reducing the thresholds.

The following topics present the detection probability in both cases. In all of these, the probability of false alarm equals  $10^{-3}$ . For a more detailed analysis of the L5 signal acquisition threshold, the reader may refer to [10].

### Pilot channel acquisition

The pilot channel is correlated with a local replica, and since there is no data present on this channel, the acquisition process is simplified because it becomes possible to integrate coherently the signal for very long period of time to acquire a complete hybrid code composed of L5 code + NH code. But unless a prior knowledge of the Doppler shift and the NH phase is available, increasing the integration time is difficult to implement because either it takes a very long time, either it requires numerous correlators.

Indeed, if the Doppler is unknown, the amount of Doppler bins that are to be explored is proportional to the integration time. Moreover, the Neuman-Hoffman correlation function degrades quickly with Doppler uncertainty, increasing the probability of wrong acquisition. To compensate that, it is possible to increase the number of non-coherent integration (to reduce noise effect), but again this penalizes the overall acquisition time.

However, once the position is known within a few hundreds of meters (less than 1 ms, in order to work in a zone around the main correlation peak, clean of any secondary lobes) and the Doppler is defined within a few Hz, the pilot acquisition shows very interesting capabilities. Typically, it can be implemented for weak signal reacquisition or acquisition once a first fix has been computed from 4 strong satellites.

The following figure illustrates the low acquisition threshold enable by pilot processing. It is assumed that the Doppler estimate allows only one frequency cell to be searched, and that position is precise enough to remove directly the Neuman-Hoffman.

Correlation losses due to Doppler and code phase uncertainties are ignored.

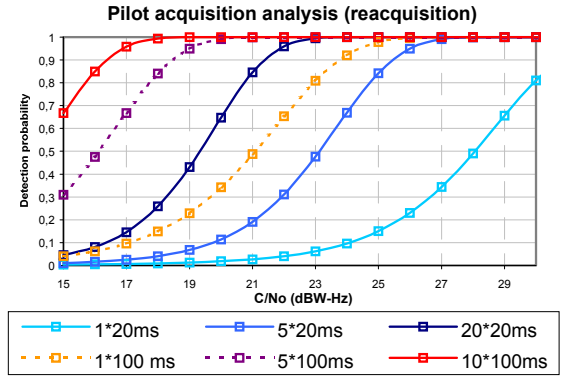


Figure 8. Pilot channel detection probability

### Dual channel acquisition

Only cold start acquisition of L5 codes (excluding NH) is being investigated here. For reacquisition processes, pilot channel computation is simpler and more performant (indeed, the presence of data on the data channel does not allow integration time higher than 10 ms). In the case of cold start, we assume that none of the following information are available: position, speed, time. For L5, the maximum Doppler uncertainty is +/-8 kHz and the code uncertainty equals the code length, i.e. 10230 chips (remind that we process first the PN code acquisition). All the frequency and code bins are to be explored.

Following our assumption, the coherent integration time is 1ms. The 1kHz correlators outputs are squared and then cumulated over M samples, thus performing a non-coherent integration of M ms. Considering the following cell width : half a code chip and 500 Hz, the worst code uncertainty is a quarter of a chip and the worst Doppler uncertainty is 250 Hz. As a consequence, the maximum losses on a 1 ms integration time are :

$$L = 20 \cdot \log(0.75) + 20 \cdot \log\left(\frac{\sin(\pi\Delta f T_p)}{\pi\Delta f T_p}\right) = -3.5 \text{ dB}$$

The total amount of cells to be searched is  $2 \cdot 10230 \cdot (32+1) = 675180$ .

The figures below show the probability of detection for dual channel acquisition. The C/No value are the composite signal-to-noise-density ratio on the antenna input.



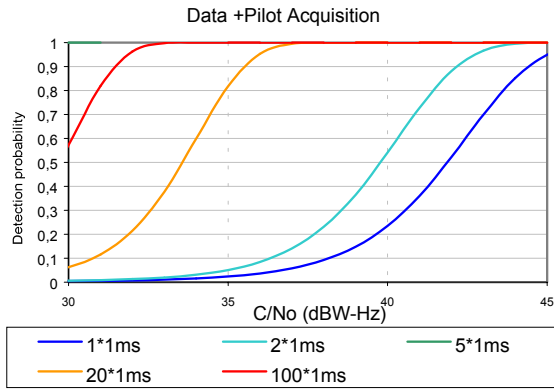


Figure 9. 1 ms acquisition data+pilot

When compared to a single channel acquisition with equivalent integration time, dual channel processing brings a 2dB improvement in acquisition threshold, or for a same threshold, reduce the acquisition time. However, for low C/No or in reacquisition process, the single channel process is far better provided the NH phase is known.

As far as cold start is concerned, L5 acquisition performance is comparable to that of L1 (except for the received power) but requires to search 10230 chips instead of 1023. At cold start, it appears difficult to extend the coherent integration because of the Neuman-Hoffman drawback (secondary lobes at 6 dB). This is unlike L1, where the coherent integration time can reach 20 ms as long as there are enough Doppler cells explored or correlators.

### SIGNAL TRACKING PERFORMANCE

As for acquisition, the tracking of GPSIIF-L5 signal, as well as any other composite pilot + data channel signal, can be performed as single channel tracking or dual channel tracking. In the case of single channel tracking, it is of course more advantageous to track the pilot channel, and to use the code and carrier phase to demodulate the navigation message.

Although dual channel tracking concerns both the code phase and the carrier phase loops, we will see in this topic that the retained strategy may differ with the type of loop (DLL or PLL). As a matter of fact, dual channel tracking significantly improve the DLL performances, but does not bring enough gain in the PLL w.r.t. complexity.

### Code tracking loop

The common expression of the noise variance of a DLL using a dot-product is

$$\sigma^2 = \lambda^2 \frac{Bn \cdot \Delta}{2 \cdot C / No} \left( 1 + \frac{Bp}{C / No} \right) \text{ (m}^2\text{)}$$

expression in which we find :

$\lambda$  is the code chip wavelength (m),

$Bn$  is the loop's equivalent noise bandwidth (Hz),

$\Delta$  is the correlator chip spacing (chips),

$Bp$  is the correlators predetection bandwidth (Hz)

$C/No$  is the signal to noise spectral density ratio (dB-Hz).

Delta's value is intimately linked to the IF bandwidth : in the case of L5 signal, the typical value of this bandwidth should be 20 or 24 MHz for aviation. Therefore, and, from now on, we will always consider that the chip spacing is equal to 1 ( lower chip spacings could may be used for applications compatible with wider bandwidth ).

The tracking threshold is usually defined from the loop noise standard deviation  $\sigma$ , the steady-state error  $\varepsilon$  and the chip spacing  $\Delta$  using the following condition :

$$3\sigma + \varepsilon \leq \frac{\Delta}{2}$$

This expression, although an approximation, is usually fairly realistic.

#### Single channel tracking : pilot channel

In the case of pilot-channel-only tracking, the above expression for the noise variance can be directly used. The noise jitter of this single channel tracking architecture is illustrated on **Figure** . The discriminator is a dot-product and the represented C/No is the total composite C/No at the antenna.

The performance obtained is very good, and as expected, the pilot channel enhances the DLL performances, even if only half of the incoming signal's power is processed. So, although simple, this architecture does not appear optimal.

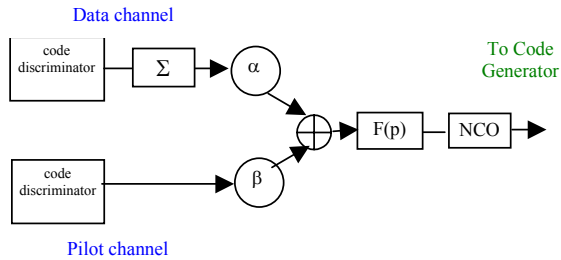
To benefit from the total incoming power, the receiver needs to track both pilot and data channel, with separate correlators and discriminators, and then to combine, in a way or another, the tracking error in order to keep a single code NCO.

### Dual channel tracking

Each of the individual discriminator function in the data and pilot channel can be combined to form a composite tracking loop. Different strategy can be implemented.

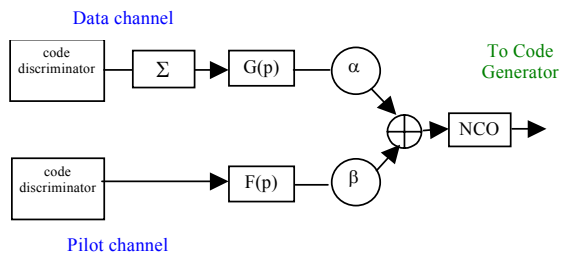
One of them [4], proposed almost as soon as the L5 specifications were drafted, consist of the weighted sum of the discriminator outputs, driving the loop filter.

The weights are calculated from the respective noise on the data and pilot channel correlators.



This technique does not only provide improved accuracy (almost a 3 dB gain at high C/No) but it does also allow for lower tracking threshold (approximately a 1 dB improvement). However, the weights applied to the data channel is such that, at low C/No, the gain provided by this technique is much lower (1 dB) than the one obtained at high C/No.

A more complex technique involves two different loop filters for the pilot and the data channels, whose outputs are combined prior to the loop NCO. The data filter features a tighter band so as to compensate the higher noise resulting from the squaring losses. The pilot filter, wider, will absorb most of the dynamics. Typical values for the individual equivalent noise bandwidth (i.e. the eq. noise bandwidth if the filter were alone in the loop) of those filter would be within a ratio of 5 or 10 (eg: 2 Hz for pilot filter and 0.4 Hz for the data).



Although more complex, this technique provides only a 1 dB improvement at low C/No compared to the previous one.

The figure below represents the tracking ability of a standalone receiver, assuming a 5 Hz loop bandwidth and a 25 Hz predetection bandwidth. The predetection bandwidth of the data channel is of course set by the symbol rate, that is 100 Hz.

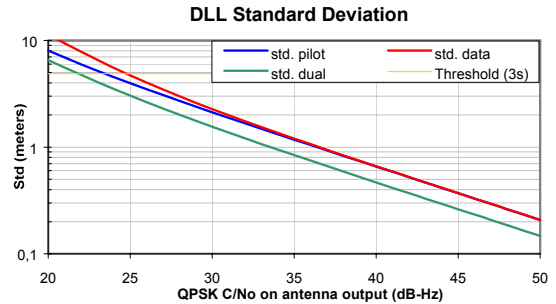


Figure 10. Code phase standard deviation for standalone DLL implementation

Using carrier-smoothing and/or external aid, such as a navigator (Kalman filter), the loop performance can be upgraded using tighter parameters. A 0.5 Hz loop bandwidth for the code loop is acceptable. As a matter of fact, the pilot predetection bandwidth highly depends on the PLL noise or on the external carrier aid provided by a navigator in so called “code-only” tracking. Yet, it can also be reduced and values of 10 Hz seems realistic since a navigator like DIOGENE (Kalman orbital navigator filter, developed by CNES) is able to provide better than 2 Hz accuracy.

Using these parameters, we can compute the standard deviation of the dot-product DLL in aided mode, again for single and dual channel tracking, the results are illustrated in Figure 11.

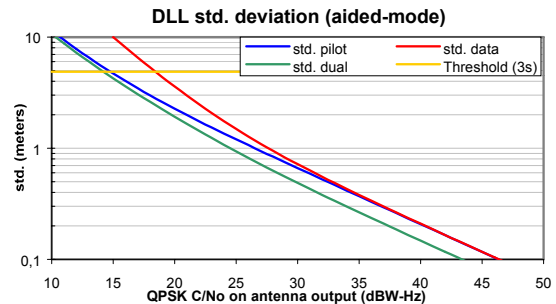


Figure 11 Code phase standard deviation for aided (and carrier smoothing) DLL implementation

In both cases, and for common values of signal-to-noise-density ratio, the pseudorange accuracy is well below one meter. The tracking threshold is below 15 dBHz (QPSK power).

## Carrier tracking loop

### Single channel tracking : taking advantage of Atan2 on pilot channel

The availability of a data-free channel affects the choice of the carrier phase discriminator (or carrier frequency discriminator in the case of a FLL). With no ambiguity left on the sign of the incoming samples (no data), the extended Atan (or Atan2) is by far the most advantageous for the pilot channel, since it offers extended linearity, and by this, extended tracking range

The noise variance of the PLL is defined as :

$$\sigma^2 = \frac{B_n}{C/no} \left( 1 + \frac{Bp}{2C/No} \right) \text{ rad}^2$$

And the tracking threshold of a Atan2 PLL on the pilot channel is  $3\sigma + \varepsilon \leq \frac{\pi}{2}$  where  $\varepsilon$  is the steady-state error of the loop.

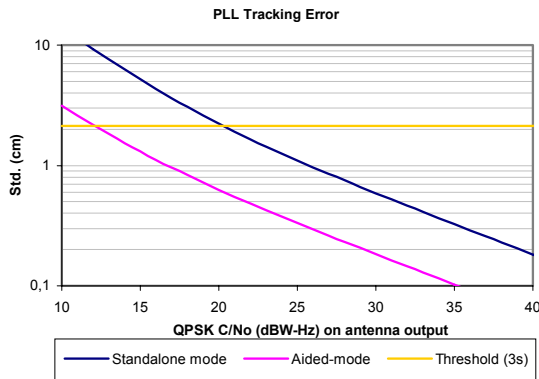


Figure 12 PLL tracking error (steady-state error =0)

### Dual channel tracking : discriminators issues[12]

When implementing channel combination on the carrier phase loop, one must take care to the jumps that may arise from a stay-state tracking error due to range dynamics inducing a wrapping of one individual discriminator.

We can build a composite discriminator function by combining a classical Atan discriminator both on the data channel and on the pilot channel. The combination is then performed using any of the techniques described for the DLL. But in order to take advantage of the data-free channel, one may also desire to combine the classical Atan on the data-channel with the extended Atan on the pilot-channel.

In that case, in order to take the full benefit of the whole operating range of the extended Atan, it is necessary to detect and correct the possible jumps of pi that may arise from the classical Atan discriminator.

A possible technique to do this is to run a step detection procedure on the difference of the data and pilot discriminators. A simple but yet efficient implementation is given in [11].

The CUSUM test is a more complex but also very efficient alternative. It could be design to test changes in the average value of the test criterion, set to be the difference of the two discriminators. Important design parameters of this CUSUM test are : the false alarm rate, the missed detection and the time to alert.

The following figure shows the lowest required C/No to guarantee the performance of the CUSUM procedure as a function of the loop noise bandwidth when the predetection time is set equal to 10 ms.

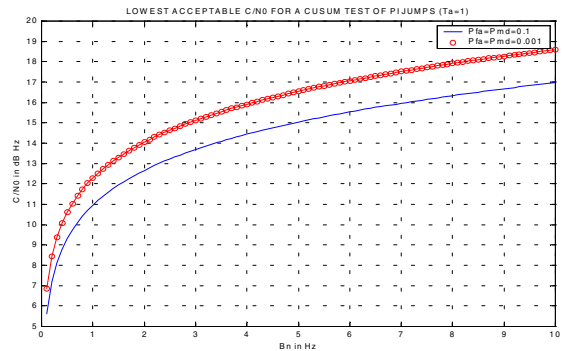


Figure 13 CUSUM TEST robustness w.r.t. loop bandwidth

With adequate definition of the probability of misdetection, the CUSUM algorithm shows very good robustness to thermal noise.

But this robustness is difficult to exploit. Indeed, the Atan discriminator is very sensible to noise. As illustrated below, the linear zone of the Atan discriminator of the data channel collapses when the squaring losses increases, to finally behave less good than a I\*Q discriminator. In comparison, the pilot discriminator keeps a fully acceptable linear zone, thanks to longer integration period and a initially double linear zone.

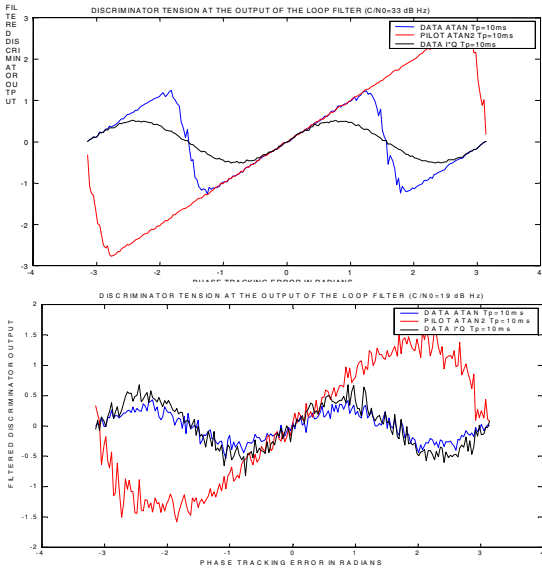


Figure 14 Atan and Atan2 discrimination function. Effect of white noise

Accounting for this, it seemed to us that tracking the carrier phase (or frequency) only on the pilot channel, using an extended Atan discriminator, seemed a more judicious choice, although probably more conservative.

### MULTIPATH MITIGATION

GPSIIF-L5 multipath mitigation performances are without surprise much better than what is usually performed with L1, even using enhanced correlators. The following figure shows the multipath error envelop for a -6dB reflected signal and a half-chip correlator spacing. For comparison, the multipath error envelop of L1 C/A with a 0,1 chip spacing is also plotted.

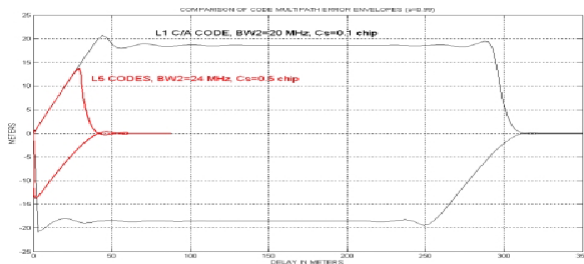


Figure 15 Multipath mitigation. Comparison with L1 C/A

The question arising is whether GPSIIF-L5 transmitted bandwidth will allow use of narrow correlators.

Although this is probably not an issue for aeronautical applications (the received bandwidth will be reduced to the main lobe, in order to reduce interference from DME/TACAN), we can easily imagine the outstanding performances one would get with a wide-band receiver using narrow correlation techniques if the L5 signal would be transmitted in 40 to 60 MHz as it is the case for the present GPS P codes (*See appendix for measured Block-*

*IIR L1 spectrum; the measurement has been ordered by CNES to ANFR, in the frame of an ANFR contract with the Leeheim earth station of RegTP)*

### IONOSPHERE AND DUAL FREQUENCIES RECEIVER

Accurate positioning requires the computation of the ionospheric delay. In single frequency receiver, it is usually done using an ionospheric model and the parameters transmitted in the navigation message.

If two frequencies are available, then the receiver can compute a ionospheric-delay free pseudorange by combining the frequency measurements. The resulting pseudorange is deteriorated by a noise, mainly the one present on the highest frequency.

In the case of a L1/L5 receiver, the good accuracy obtained on L5 is affected by the higher noise on the L1 pseudorange. In addition to that, the tracking threshold of L5 being lower than the one of L1, the receiver might loose its ionospheric correction capability as the C/No degrades.

$$d = \frac{psd_1 - \Gamma psd_5}{1 - \Gamma} \quad \text{with} \quad \Gamma = \frac{f_5^2}{f_1^2}$$

$$\sigma_d^2 = \frac{1}{(1 - \Gamma)^2} (\sigma_1^2 + \Gamma^2 \sigma_5^2)$$

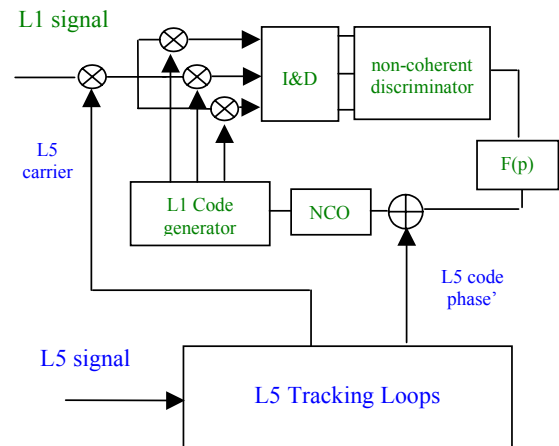


Figure 16 Example of combined L5/L1 tracking

In such cases, aiding the L1 tracking with the L5 NCOs command can substantially upgrade the overall performances. The dynamics seen by the L1 DLL is mainly reduced to the ionospheric dynamics, thus allowing for loop bandwidth below 1 Hz.

This architecture can also help reducing the receiver complexity. Indeed, by using only non-coherent

discriminator like the dot-product, only one carrier NCO, tracking the L5 pilot, is necessary (it is assumed that the ionospheric Doppler drift is lower than 50 Hz, the maximum predetection bandwidth of L1).

**Figure 17** illustrates the standard deviation on the measured iono-free distance after dual-frequency processing. Those results take into account a L1 received-power 3 dB below the QPSK power of L5 (assuming that L1's C/A effective minimum power received on the ground is  $-157$  dBW instead of  $-160$  dBW). The case of single frequency processing (L5) with an ionospheric model is also shown, though that particular case, the error is rather a bias.

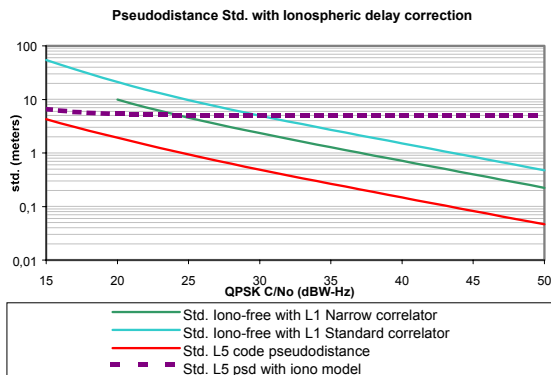


**Figure 17 L5/L1 ionospheric corrections**

The threshold is not such an issue as the accuracy, at least as long as carrier ambiguity techniques are not used. Indeed, at low C/No, the L1 accuracy is worse than the accuracy the ionospheric model would provide (5m at  $1\sigma$ ). So at low C/No, a single frequency mode is preferable since the L5 pseudorange measurement, coupled to the ionospheric model, gives better results.

**APPLICATION EXAMPLE : GEO STATIONARY PLATFORM**

Simulations were run to calculate the number of satellites tracked by a L5 receiver on-board a geostationary satellite. Cold start acquisition is considered to calculate the number of tracked satellite at the simulation start. Then, only warm acquisition or reacquisition is taken into account.

Relying on the results above regarding cold start acquisition, we will assume a cold start acquisition threshold of 30 dBHz.

Once a first PVT solution is available, the orbital navigator can estimate the dynamic and position of yet untracked satellite, using for example the almanach. This leads to the NH ambiguity resolution, enabling integration time longer than 20 ms. Moreover, the navigator is able to produce a Doppler estimation within a few Hz. In such

condition, coherent integration time of 100 ms are possible, leading to a realistic acquisition threshold of 20 dBHz.

Finally, we have to define what a reasonable tracking threshold is. Again, the use of a navigator to push the loops NCOs (both PLL and DLL) will help dealing with longer predetection time and narrow loop filter.

As a matter of fact, considering the performances awaited with a navigator like DIOGENE-2 for L1C/A, values of 1 Hz for the code loop bandwidth and of 2 Hz for the carrier loop bandwidth appear realistic. For the DLL, one can even expect values of 0,1 Hz. The code loop thresholds is thus below 15 dBHz.

And with a carrier loop bandwidth of 1 Hz, single channel extended arctan carrier tracking on the pilot channel and predetection bandwidth of 10 Hz, the carrier loop thresholds is around 12 dBHz.

The tracking threshold is set to the highest of those two previous values, that is, 15 dBHz.

The following results represent the GTO orbit, usually the worst case for Geo GPS receiver.

The simulation assumptions regarding the L5 link budget are :

EIRP is such that the receive power on ground for a  $5^\circ$  elevation is  $-157$  dBW per component.

Antenna pattern is identical to L1. It is assumed that the L5 antenna will be a iso-flux antenna.

The receiver noise figure is set to 3 dB, resulting a No value of  $-200$  dBW/Hz.

For comparison, the results for L1 GPS receiver TOPSTAR 3000 scheduled to flight onboard STENTOR by the end of this year are also represented. As reference, the total amount of visible satellites (i.e. not masked by the earth), is also illustrated.

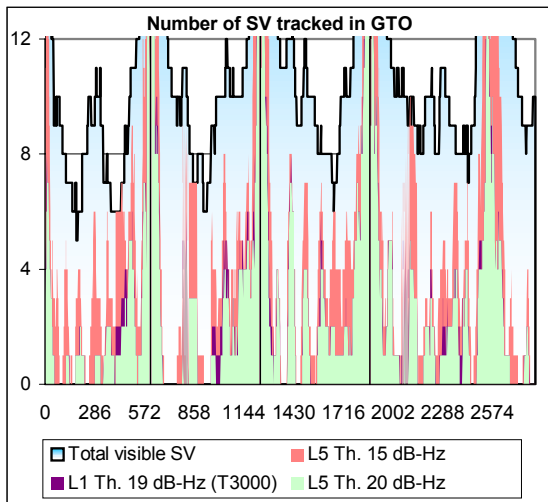


Figure 18 Applying L5 tracking to geostationary receivers

It appears clearly on this graph that the amount of tracked satellite increases. The time during which the number of GPS SV is above 4 is increased by almost 100 %.

## CONCLUSIONS

As a conclusion, the L5 signal shows some interesting properties. As far as cold-start acquisition is concerned, the Neuman-Hoffman limits the coherent integration time to 1 ms whereas it can be of 20 ms for L1 C/A. This limitation should not be an issue for aviation, but should be studied more deeply for other applications.

The L5 codes properties were also studied and their effect on interference on Galileo E5a signal were put in evidence. These results highlighted that L5/E5A compatibility issue has to be assessed more deeply since a coordination appears to be necessary for GPS-L5 to overlay E5a. The optimization of a GPS and Galileo E5a code family could solve this problem.

## ACKNOWLEDGEMENT

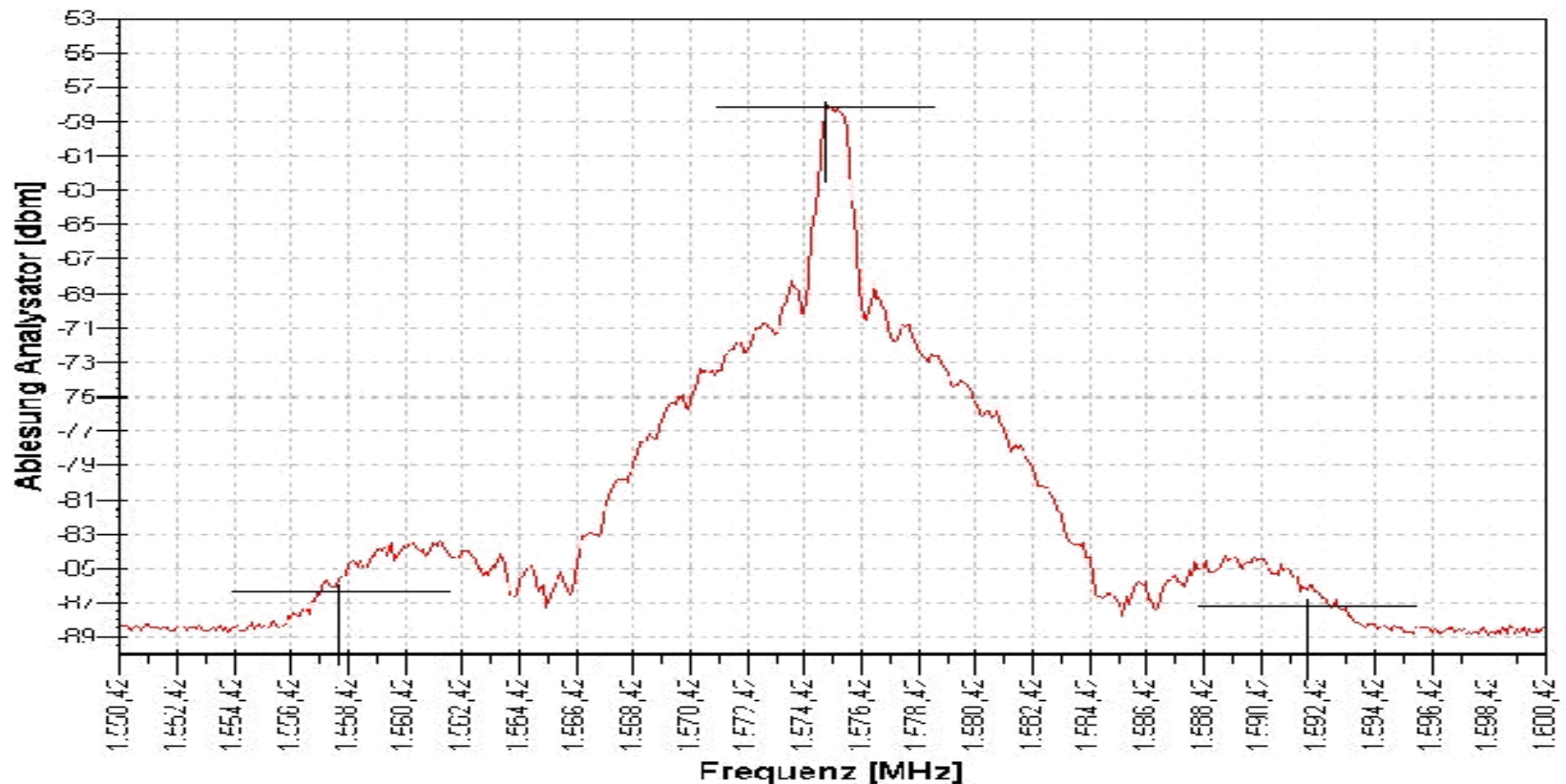
Acknowledgement is made for the helpful and constructive co-operation between CNES, TéSA and M3Systems, that lead to the analysis presented here.

The views and concepts expressed herein represent those of the authors and do not imply any official recognition or application by any organisation with which the author is associated.

## REFERENCES

- [1] "GPS Principles and Applications" [Kaplan., 1996], E. Kaplan, Artech House
- [2] "NAVSTAR GPS L5 Signal Specifications", Anon., , RTCA, December 2000
- [3] "Proposed New Civil GPS Signal at 1176.45 MHz", [Spilker and Van Dierendonck., 1999], J. Spilker, A.J. Van Dierendonck, ION GPS 1999
- [4] "Evaluation of the proposed Signal Structure for the New Civil GPS Signal at 1176.45 MHz", [Hegarty., 1999], C. Hegarty, The MITRE Corporation, Working Note WN99W34, June 1999
- [5] "A L5 Receiver Test Bench", Ries L., Dantepal J., JL. Issler, Proceedings of The Institute of Navigation ION GPS-2001
- [6] « L5 Codes Properties », [Macabiau et al., 2002], C. Macabiau, V. Calmettes, W. Vigneau, L. Ries, J-L. Issler, GNSS'2002. Copenhagen
- [7] "Assessing the Radio Frequency Compatibility between GPS and Galileo", J. Godet, J. C. de Mateo, P. Erhard, O. Nouvel.
- [8] "GPS/Galileo Radiofrequency Compatibility Analysis", J. Godet, CNES/GAST ION GPS Sept. 2000.
- [9] "GPS/Galileo interference analysis, Cross-correlation and Doppler analysis in L1", O. Nouvel, J. Godet, JL. Issler. CNES technical note. DTS/AE/TTL/RN/2001-061. 25/07/01.
- [10] "Analysis of E5/L5 acquisition, tracking and data demodulation thresholds" [Bastide et al., 2002], F. Bastide, O. Julien, C. Macabiau, B. Roturier, , ION GPS 2002
- [11] "Receiver Algorithms for the New Civil GPS Signals", [Tran and Hegarty., 2002], M. Tran, C. Hegarty, ION NTM 2002
- [12] "L5 Receiver implementation issues", Macabiau C. , Ries L. ,CNES Technical Note, September 2002
- [13] " CCT TSI. CNES Workshop. Interoperability of GNSS Signals. Toulouse, 29/30 November 2001". CNES report DTS/AE/TTL/RN – 02/033. J-L. Issler

APPENDIX : MEASURED BLOCK-HIR SPECTRUM



*Belegte Bandbreite nach VOF 147 (R/2=0.5 %): 34.17 MHz  
 Mitte der berechneten Bandbreite: 1575.3198 [MHz]  
 Untere Frequenz/Pegel: 1559.20560 MHz/-85.6 dBm  
 Mittlere Frequenz/Pegel: 1575.36990 MHz/-58.1 dBm  
 Obere Frequenz/Pegel: 1592.40397 MHz/-86.3 dBm*

Datum Uhrzeit : 27.09.02 08:41:59  
 Mittel-Frequenz: 1575.4200 [MHz] Span: 50.0000 [MHz]  
 Analysator : R&S FSIQ Betriebsart :  
 Messtiler : 200 kHz Videofilter : kHz Überlautzeit : 640.00 [msec]